[Article ID] 1003- 6326(2002)02- 0297- 04

# Microstructure and interface fracture of LPPS Ni/Fe and Cu/Ni sprayed materials①

LI Dong-fei(李东飞), SHAO Bei-ling(邵贝羚), LIU An-sheng(刘安生),
AN Sheng(安 生), ZHU Qi-fang(朱其芳)
(General Research Institute for Non-ferrous Metals, Beijing 100088, China)

[Abstract] The interfaces of two materials, Ni/Fe and Cu/Ni, deposited by low pressure plasma spraying method, were studied by means of scanning electron microscopy (SEM) and transmission electron microscopy (TEM) combined with energy dispersive X-ray spectroscopy (EDS). The adhesion between coatings and substrates was measured with the aid of Knoop interfacial indentation testing method. The results show that the interfacial microstructures have strong influence on the mechanical properties. Cu/Ni interface is weak link with NiO amorphous phase. Ni/Fe interfacial layer consists primarily of Fe and Ni oxide crystalline phases, containing dispersive (Fe, Ni) spotlike intermetallic compound phase in nanometer dimension, and the interfacial interdiffusion was detected. The micro-mechanism of interfacial fracture was discussed.

[Key words] microstructures; interfacial bonding strength; low-pressure plasma spraying; amorphous phase
[CLC number] TG 146.1 [Document code] A

## 1 INTRODUCTION

Plasma spraying, developed from combustion flame spraying, is now a well-established widely used process for coating metals with almost any materials (metallic, ceramic and polymeric) which can be melted without decomposition or excessive vaporization in the plasma jet[1]. Many related reports have been published[2~15]. All these studies on coatings and sprayed interface put more emphases on macro-fracture mechanics rather than micro-mechanism from interfacial microstructure. There is less understanding on the relationship between microstructure and mechanism of fracture. In the present work, the microstructural characterization of interface for two sprayed materials, Ni/Fe and Cu/Ni, deposited using low-pressure plasma spraying (LPPS) method, was studied. The interfacial fracture and related factor from interfacial microstructure were issued.

## 2 EXPERIMENTAL

The LPPS spraying was carried out using a DY-DP-1 equipment. Two starting powders were commercially available Cu and Ni metals powder with size range of 20~ 70 μm. Cu powder was sprayed on industrial pure nickel plate and Ni on industrial pure iron plate respectively. Before spraying, two substrates were cleared using transferred arc to remove their surface oxide. Process parameters used in the experiment are listed in Table 1.

**Table 1** Low-pressure plasma spray parameters of Cu and Ni coatings

| LPPS parameters | Cu coating | Ni coating |
|---|---|---|
| Voltage/V | 50~ 60 | 60~ 75 |
| Current/A | 300~ 400 | 200~ 300 |
| Spray distance/m | 0.2~ 0.3 | 0.2~ 0.3 |
| Vacuum chamber pressure/MPa | 0.01~ 0.03 | 0.01~ 0.03 |
| Powder feed rate/(g·min$^{-1}$) | 20~ 40 | 20~ 40 |
| Primary gas (argon) /(MPa/SLM) | 0.4/40~ 50 | 0.4/40~ 50 |
| Secondary gas (hydrogen) /(MPa/SLM) | 0.4/2~ 5 | 0.4/2~ 5 |

In order to measure the interfacial bonding property, the cross-sectional specimens for Knoop interfacial indentation test were prepared. The Knoop indenter was loaded and then unloaded continuously on the interface between the coating and substrate until the interface cracked. The interfacial bonding property was achieved by calculating the interfacial fracture specific energy. The more the interfacial fracture specific energy, the higher the interfacial bonding strength[16].

The paper was concerned with establishing the microstructural characteristics of the interface between the substrate and the coating. Thus, special specimen techniques were developed for preparing proper interfacial specimens for examination in TEM[16]. JSM-840 SEM and JEM-2000FX TEM

① [Foundation item] Project (59971013) supported by the National Natural Science Foundation of China
[Received date] 2001- 05- 25; [Accepted date] 2001- 07- 09

with VOYAGER 3105 EDS were used to study the interfacial morphology, microstructure and microcomposition.

## 3 RESULTS AND DISCUSSION

### 3.1 Interfacial bonding property

The detected values of interfacial bonding property for Ni/Fe and Cu/Ni by Knoop interfacial indentation are listed in Table 2. The results show that the interfacial fracture specific energy of Ni/Fe is about 14 times of that of Cu/Ni, which means that the interfacial bonding strength of Ni/Fe is much higher than that of Cu/Ni.

**Table 2** Interfacial bond strength of Ni/Fe and Cu/Ni

| Specimen | Interfacial fracture specific energy/($N \cdot mm^{-1}$) | Interfacial bonding strength |
|---|---|---|
| Ni/Fe | 10.88 | High |
| Cu/Ni | 0.76 | Low |

### 3.2 Interfacial microstructure

Fig. 1(a) and (b) are SEM micrographs showing cross-sectional microstructure of Ni/Fe and Cu/Ni, respectively. It can be found that there exist many unmelted nickel spherical particles in the Ni coating and the coating bonds well with the Fe substrate. However, in Cu coating is almost fully molten copper. Some microcrackings exist close to the interface, as shown by the arrows in Fig. 1(b).

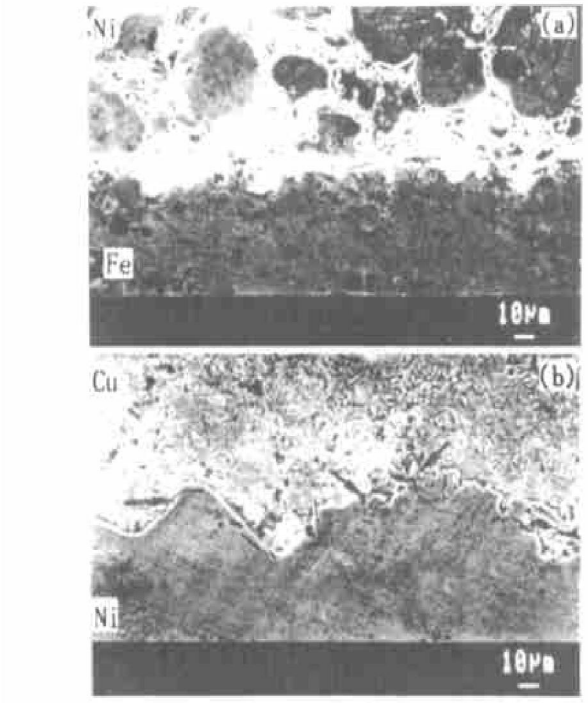


**Fig. 1** SEM micrographs, showing section of (a) Ni/Fe, (b) Cu/Ni

A TEM micrograph of the Cu/Ni interfacial region is shown in Fig. 2, from which it can be seen that there is a lay of amorphous phase with a varying width from 100 mm to 400 nm between the nickel substrate and polycrystalline copper coating.

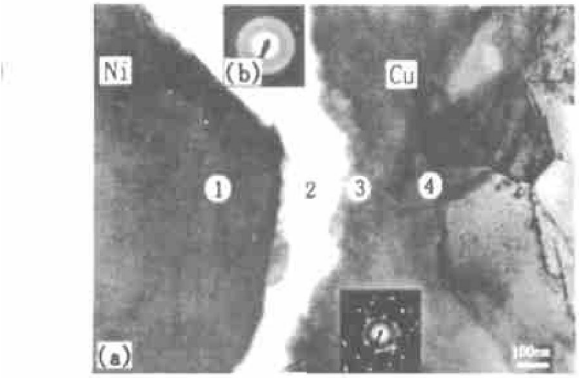


**Fig. 2** Interfacial TEM image (a) of Cu/Ni and SAD pattern (b) of Cu/Ni interface

The TEM EDS spectra were collected from different region, as marked circle 1, 2, 3 and 4 in Fig. 2. These spectra show that the amorphous phase is NiO phase and no obvious element diffusion occurs adjacent to the Cu/Ni interface.

The Ni/Fe interface is platelike structure, as shown in Fig. 3. The selected area diffraction (SAD) patterns from different regions of Ni/Fe interface are shown in Fig. 4.

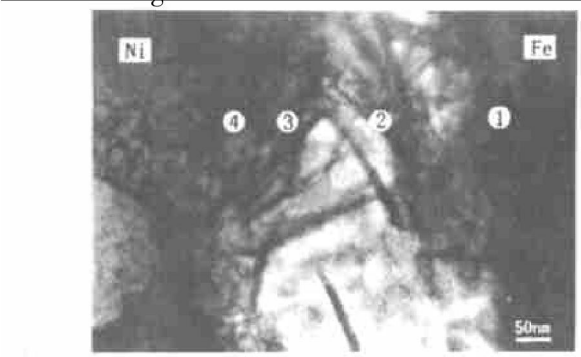


**Fig. 3** Interfacial TEM image of Ni/Fe

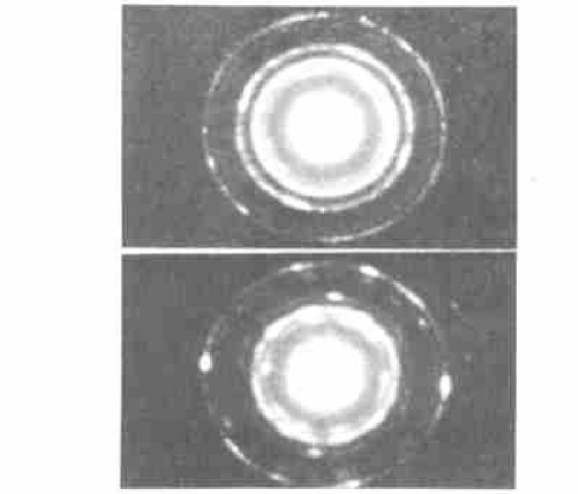

**Fig. 4** Selected area diffraction patterns of different regions on Ni/Fe interface

The Ni/Fe interfacial phases identified using these SAD patterns are oxide crystalline phase of Ni and Fe ($NiFe_2O_4$, $Fe_2O_3$) and (Fe, Ni) intermetallic compound phase. The dark field image analysis makes sure that the platelike structure is oxide crystalline phase of Fe and Ni and dispersive (Fe, Ni) spotlike intermetallic compound phase in nanometer dimension is distributed in the oxide phase.

The TEM EDS spectra from different regions of Ni/Fe marked circle 1, 2, 3 and 4 in Fig. 3 suggest that a composition transition from the Ni-rich coating to the Fe-rich substrate occurs across the interface.

### 3.3 Discussion

3.3.1 Interfacial phases and interfacial diffusion

The interface of Cu/Ni was consisted of single NiO amorphous phase. While spraying, the molten copper particles struck onto nickel substrate and spread along its surface. As the high thermal conductivity of copper, the CuO was quenched to substrate temperature in a short time. Thus the CuO amorphous phase was produced. Because of higher affinity of nickel with oxygen than copper at high-temperature, nickel would reduce the copper from the CuO to produce stable NiO amorphous phase. This NiO amorphous phase prevented copper and nickel element from interdiffusion. Moreover, with molten copper particles striking onto the nickel substrate, a pancake shape was obtained. The heat in the pancake droplet was dissipated over a much greater area of the Ni substrate and it was likely that melting of Ni substrate would be less. The kinetic energy of the droplet was also dissipated by the sideways flow of the liquid phase. Thus it is not surprising that a weakly interfacial bonding is expected and found in fact.

As to Ni/Fe specimen, the oxide phase of Ni and Fe was crystalline due to the low thermal conductivity of nickel. There were many unmelted nickel particles in the Ni coating, as shown in Fig. 1(a). As the heat flowed from this spherical droplet over a much smaller area into the iron substrate, the iron melted partially and the molten iron could then react chemically with molten nickel to produce (Fe, Ni) intermetallic compound phase. Thus, it formed partially metallurgical bonding between the Ni coating and the Fe substrate. It also was remembered that the high kinetic energy of the unmelted droplet also has to be transferred when it strikes the interface and this could also enhance the bonding.

3.3.2 Interfacial fracture

The interfacial microstructures produce predominant effect on the interfacial crackings initiation and propagation. As to the Ni/Fe interface, the dispersive (Fe, Ni) nano-crystals were obstacle for the interfacial cracking propagation by absorbing their energy or changing their extension direction. Fig. 5 is a schematic illustration showing how the cracking extends in the intercrystalline and intracrystalline direction.

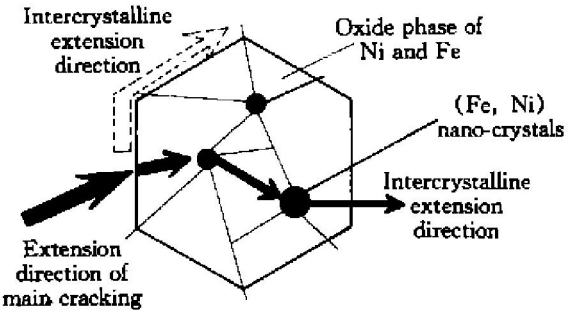


**Fig. 5** Schematic illustration of cracking extension in intercrystalline and intracrystalline direction

When the cracking occurred, it could extend into the grain or along the grain boundary of the oxide phase of Ni and Fe. The stress on the interface between the (Fe, Ni) nano-crystals and oxide phase of nickel and iron brought about some potential micro-crackings around the (Fe, Ni) nano-crystals, which made these regions weak relatively. While the main cracking extended further, the micro-crackings on the tip the main cracking would absorb the strain energy to decrease the stress concentration. As a result, the (Fe, Ni) nano-crystals stopped the cracking from extending further or changed its extension direction. Additionally, the oxide crystalline phase included some plastic zones, the strain hardening within the plastic zone raised the stress intensity level for further deformation, consequently decreased the crack growth rate.

As for the Cu/Ni interface, the single NiO amorphous phase was brittle relatively and had no strengthening effect like the (Fe, Ni) nano-crystals. Once the crack occurred, it would propagate quickly through the whole interface.

## 4 CONCLUSIONS

1) The interfacial bonding property has close relationship with its interfacial microstructure. The Cu/Ni interface is weak link with NiO amorphous phase. No interfacial interdiffusion occurs.

2) The Ni/Fe interface is strong link with interfacial layer consisting primarily of Fe and Ni oxide crystalline phase and dispersive (Fe, Ni) spotlike intermetallic compound phase in nanometer dimension. The interfacial interdiffusion was detected.

3) The Ni/Fe interface has more effective inhibition to interface cracking extension than that of Cu/Ni interface.

## [REFERENCES]

[1] Mcpherson R. The relationships between the mechanism

of formation, microstructure and properties of plasma sprayed coatings [J]. Thin Solid Films, 1981, 83: 297 – 310.

[2] Hsu I C. Wu S K. Oxidation improvement of Ti-48Al-2Cr-2Nb intermetallics by air plasma sprayed $ZrO_2$-Ni-4.5(wt)% Al coating [J]. Surf Coat Technol, 1997, 90: 6 – 13.

[3] XIANG Xin-hua, ZHU J C, YIN Z D, et al. Fabrication and microstructure of $ZrO_2$/NiCrAlY graded coating by plasma spraying [J]. Surf Coat Technol, 1997, 88: 66 – 69.

[4] Mcpherson R. A model for the thermal conductivity of plasma sprayed ceramic coatings [J]. Thin Solid Films, 1984, 1: 89– 95.

[5] Pajares A, Wei Lan-hua, Lawn B R, et al. Mechanical characterization of plasma sprayed ceramic coatings on metal substrates by contact test [J]. Materials Science and Engineering, 1996, A 208: 158– 165.

[6] Mcpherson R, Shafer B V. Interlamellar contact within plasma sprayed coatings [J]. Thin Solid Film, 1982, 97: 201– 204.

[7] Brtlett A H, Maschio R D. Failure mechanism of a zirconia-8wt% yttria thermal barrier coating [J]. J Am Ceram Soc, 1995, 8(4): 1018– 1024.

[8] Wayne S F. Sampath S. Structure/property relationship in sintered and thermally sprayed WC-Co [J]. J Therm Spray Technol, 1992, 1(4): 307– 316.

[9] Sampath S, Neiser R A. A structural investigation of a plasma sprayed Ni-Cr based alloy coating [J]. J Mater Res, 1993, 8(1): 78– 86.

[10] Murakami K. Okamoto T. Structure and mechanical properties of a thermal-sprayed Nickel-20wt.% chromium alloys [J]. Mater Sci Eng A, 1993, A160(2): 181 – 187.

[11] Richard C S, Beranger G. Study of $Cr_2O_3$ coatings. 1. Microstructures and modulus [J]. J Therm Spray Technol, 1995, 4(4): 342– 346.

[12] Newaz G, Nusier S. Analysis of interfacial cracks in a TBC/superalloy system under thermal loading [J]. Eng Fract Mech, 1998, 60(5– 6): 577– 581.

[13] El-shazly M H, El-sherbiney M. The effect of hard coating properties on substrate stresses under tribological loads [J]. Mater Manuf Process, 1999, 14(2): 243– 255.

[14] Izdinsky K, Ivan J. Microstructure of the as-plasma sprayed NiCrAlY coating [J]. Kovove Mater, 1998, 36(5): 367– 377.

[15] Unal O, Akinl M. Strength measurement of thick brittle coatings on metals [J]. Ceram Eng Sci Proc, 1998, 19(4): 283– 291.

[16] LI Dong-fei. Study on Micro-Mechanism for Interfacial Fracture of Coating Composite. MS Dissertation (in Chinese), [M]. Beijing: General Research Institute for Non-ferrous Metals, 2001.

**(Edited by HE Xue-feng)**